ATMOSPHERIC CONVECTION WITH CONDENSATION OF THE MAJOR COMPONENT.

T. Yamashita, *Department of Cosmosciences, Hokkaido University, Japan (yamasita@ep.sci.hokudai.ac.jp)*, **M. Odaka,** *Department of Cosmosciences, Hokkaido University, Japan*, **K. Sugiyama,** *Center for Planetary Science(CPS) / Institute of Low Temperature Science, Hokkaido University, Japan*, **K. Nakajima,** *Department of Earth and Planetary Sciences, Faculty of Sciences, Kyushu University, Japan*, **M. Ishiwatari,** *CPS / Department of Cosmosciences, Graduate School of Science, Hokkaido University, Japan*, **Y.O. Takahashi,** *CPS / Department of Earth and Planetary Sciences, Kobe University, Japan*, **Y.-Y. Hayashi,** *CPS / Department of Earth and Planetary Sciences, Kobe University, Japan*.

Introduction

In Martian atmosphere, atmospheric major component, CO_2, condenses. In current Martian polar regions, CO_2 ice clouds are known to exist, and there is a possibility that these clouds are formed by convective motion (Colaprete *et al*., 2003). Pollack *et al*.(1987) and Kasting(1991) proposed that the early Martian atmosphere was thicker than present one, and that large amounts of CO_2 ice cloud existed. Studies on the early Martian climate suggested that the scattering greenhouse effect of CO_2 ice clouds had a significant effect on the climate (Forget and Pierrehumbert, 1997: Mitsuda, 2007).

In a system whose major component condenses, the degrees of freedom for thermodynamic variables degenerate when supersaturation does not occur. Due to degeneracy of degree of freedom, temperature profile of ascent region must be equal to that of descent region, and air parcel can not obtain buoyancy. Colaprete *et al*. (2003) performed calculations and showed that moist convection develops when supersaturation occurs, because the supersaturation will permit the temperature profile to deviate from the thermodynamical equilibrium. Laboratory experiments and observations from orbiters suggested existence of highly supersaturated regions in Martian atmosphere (Glandorf *et al*., 2002: Colaprete *et al*., 2003).

However, the model used by Colaprete *et al*. (2003) was vertical one dimensional, and there was an uncertainty in the parameterizations related to the effects of entrainment and pressure gradient. In order to investigate atmospheric convective structure in various planets, we have been developing a two-dimensional cloud convection model (e.g., Nakajima *et al*, 2000: Odaka *et al.*, 2006: Sugiyama *et al.*, 2009). Odaka *et al.* (2006) incorporated the effects of condensation of major component into the cloud convection model, and performed numerical experiments of ascending hot plume as a test calculation under Martian atmospheric condition. We incorporated a simple radiation scheme in which heating and cooling is balanced, and improve the condensation scheme in order to allows for supersaturation to occur. In this study, we perform a long-time numerical simulation of convection with condensation of the major component using the cloud convection model. In our calculation, the critical saturation ratio S_{cr} is set to be 1.0. The purpose of this study is to investigate cloud structure in statistical equilibrium states and whether moist convection can develop in the case of $S_{cr} = 1.0$.

Model description

We assume that atmosphere consists entirely of CO_2. The governing equations are the quasi-compressible equations by Klemp and Wilhelmson(1978) with additional terms representing major component condensation (Odaka *et al.*, 2005). The model is two-dimensional in the horizontal and vertical directions. The equations of motion, the pressure equation, the thermodynamic equation, and the conservation law for cloud are written as

$$\frac{du'}{dt} = -c_p\overline{\theta}\frac{\partial \pi'}{\partial x} + D_m(u'), \tag{1}$$

$$\frac{dw'}{dt} = -c_p\overline{\theta}\frac{\partial \pi'}{\partial z} + g\frac{\theta'}{\overline{\theta}} + D_m(w'), \tag{2}$$

$$\frac{\partial \pi'}{\partial t} + \frac{R\overline{\pi}}{c_v\overline{\rho}\overline{\theta}}\left[\frac{\partial(\overline{\rho}\overline{\theta}u')}{\partial x} + \frac{\partial(\overline{\rho}\overline{\theta}w')}{\partial z}\right] = \frac{R\overline{\pi}}{c_v\overline{\rho}}\left(\frac{L}{c_p\overline{\theta}\overline{\pi}} - 1\right)M_c + \frac{R}{c_v\overline{\theta}}\left(Q_{dis} + Q_{rad}\right), \tag{3}$$

$$\frac{d\theta'}{dt} + w'\frac{\partial\overline{\theta}}{\partial z} = \frac{1}{\overline{\pi}}\left(\frac{LM_c}{\overline{\rho}c_p} + Q_{dis} + Q_{rad}\right) + D_h(\theta'), \tag{4}$$

$$\frac{\partial \rho_s'}{\partial t} + \frac{\partial(\rho_s'u')}{\partial x} + \frac{\partial(\rho_s'w')}{\partial z} = M_c + D_h(\rho_s), \tag{5}$$

where

$$\frac{d}{dt} = \frac{\partial}{\partial t} + u'\frac{\partial}{\partial x} + w'\frac{\partial}{\partial z}, \tag{6}$$

$$D_*(\cdot) = \frac{\partial}{\partial x}\left[K_*\frac{\partial(\cdot)}{\partial x}\right] + \frac{1}{\overline{\rho}}\frac{\partial}{\partial z}\left[\overline{\rho}K_*\frac{\partial(\cdot)}{\partial z}\right]. \tag{7}$$

u and w are horizontal and vertical component of velocity, respectively. ρ is gas density, ρ_s is cloud density, and T is temperature. π is the Exner function: $\pi = (p/p_0)^{R/c_p}$, where p is pressure, and p_0 is surface pressure. θ is potential temperature: $\theta = T/\pi$. Overbar denotes the basic state which depends only on height, and prime denotes the perturbation component. K_m and

K_h are eddy coefficients for momentum and scalar variables, respectively. Q_{dis} is heating rate of dissipation. K_m, K_h and Q_{dis} are calculated by using 1.5 order closure (Klemp and Wilhelmson, 1978). Q_{rad} is radiative heating rate, M_c is condensation rate, and L is latent heat of fusion. c_p and c_v are the specific heat at constant pressure and volume, respectively. R is the gas constant for unit mass, g is gravitational acceleration.

We do not calculate radiation transfer explicitly, but we give horizontally uniform heating and cooling. Cooling rate is fixed at constant value q_{cool}, and heating rate $q_{heat}(t)$ is adjusted to retain $\int_{z_b}^{z_t} \rho Q_{rad} dz = 0$, where z_b, z_t are lower and upper levels of computational domain. Then Q_{rad} is given by

$$Q_{rad}(z,t) = \begin{cases} q_{heat}(t), & (z_1 \le z \le z_2) \\ q_{cool}, & (z_3 \le z \le z_4) \\ 0, & (otherwise) \end{cases} \tag{8}$$

where z_1, z_2 are lower and upper levels of cooling layer, and z_3, z_4 are lower and upper levels of heating layer. $q_{heat}(t)$ is given by

$$q_{heat}(t) = -q_{cool} \times \frac{\int_{z_3}^{z_4} \rho dz}{\int_{z_1}^{z_2} \rho dz}. \tag{9}$$

Neither surface fluxes of momentum nor heat are considered in our model.

Condensation of CO_2 occurs when saturation ratio $S = p/p_*$ exceeds critical saturation ratio S_{cr}, where p_* is saturated vapor pressure. p_* is given by

$$p_* = \exp\left(A_{ant} - \frac{B_{ant}}{T}\right), \tag{10}$$

where $A_{ant} = 27.4$, $B_{ant} = 3103$ K (The society of chemical engineers of Japan, 1999). We assume that cloud particles grow by diffusion process, and the growth by coalescence process is not considered. M_c is expressed by Tobie *et al.* (2003)'s formulation with a threshold for inhibiting unphysical condensation;

$$M_c = \frac{4\pi r N k_d R T^2}{L^2}(S-1) \quad \text{if} \quad \begin{cases} S > S_{cr} \\ or \;\; S \le 1, \rho_s \ne 0 \\ or \;\; 1 < S \le S_{cr}, \rho_s > \varepsilon, \end{cases} \tag{11}$$

where r is cloud particle radius(determined by (12)), N is number density of condensation nuclei, and k_d is heat conduction coefficient. We use the value of $k_d = 4.8 \times 10^{-3}$ W K^{-1} m^{-1} (Tobie *et al.*, 2003). ε is a threshold constant for inhibiting unphysical condensation which can occur when S is large. From (10) and the Clausius-Clapeyron equation, L is constant value: $L = B_{ant}R$.

We assume that r in one grid domain are constant, and r is expressed by ρ_s' and r_d :

$$r = \left(r_d^3 + \frac{3\rho_s'}{4\pi N \rho_I}\right)^{1/3}, \tag{12}$$

where ρ_I is the density of CO_2 ice. ρ_I is 1.565×10^3 kg/m^3 (NAOJ, 2004), r_d is 0.1 μm, and number of condensation nucleus per unit mass of air $N/\overline{\rho}$ is 5.0×10^8 kg^{-1} (Tobie *et al.*, 2003).

In this simulation, we do not consider falling of cloud particle and drag force due to cloud particles.

For space discretization, we use fourth order centered difference for advection terms, and second order centered difference for the other terms. Solving the advection term of cloud density by using centered difference causes negative cloud density. When negative cloud density occurs in a grid point, positive cloud density is transferred from surrounding points to the point so that the cloud density at the point is zero.

For saving computational resources, time-splitting method is used. The terms associated with sound wave and condensation are treated by the HE-VI scheme using a short time step. In the horizontal and vertical direction, Euler and Crank-Nicolson scheme are used, respectively. The other terms are treated by the leap-frog scheme with Asselin time filter(Asselin, 1972) using a long time step. The filter coefficient is 0.1. Artificial viscosity terms are introduced for the sake of calculation stability.

Developed numerical models and documents are available in http://www.gfd-dennou.org/library/deepconv/.

Numerical configuration

The computational domain is 50 km in the horizontal direction and 20 km in the vertical direction. Grid spacing is 200 m. Short time step is 0.125 sec, and long time step is 1.0 sec. We set surface pressure and temperature to be 7 hPa and 165 K, respectively. We use periodic boundary condition in horizontal direction and stress-free boundary condition in vertical direction. We give an initial temperature profile on the basis of a temperature profile in Martian winter polar cap (Colaprete and Toon, 2002). In this profile, temperature follows the dry adiabatic lapse rate below 4 km height, and follows the saturated vapor pressure from 4 km height to 15 km height, and is nearly constant (134 K) above 15 km height (Fig.1 left). The initial pressure profile is determined by the hydrostatic equation. As initial perturbation, random noise of potential temperature with amplitude of 1 K is added to the lowest layer of atmosphere. As for the radiation profile, we give $z_1 = 0$ km, $z_2 = z_3 = 1$ km, $z_4 = 15$ km, and $q_{cool} = -5.0$ K/day (Fig.1 right). S_{cr} in our calculation is 1.0. Integration time is 8.64×10^5 sec (10 days).

Results

In our calculation, it seems that a quasi-equilibrium state is obtained at about 3.0×10^5 sec. Total cloud mass increases monotonically until about 3.0×10^5 sec, and thereafter it is nearly constant temporally (Fig.2). Total kinetic energy also increases monotonically until

about 3.0×10^5 sec, and it is nearly constant after the time(Figure not shown).

We describe here time evolution of cloud density and vertical velocity. Fig.3a, 3b and 3c show distributions of cloud density at 2.16×10^4, 8.64×10^4 and 3.03×10^5 sec, respectively. Fig.4a, 4b and 4c show distributions of vertical velocity at 2.16×10^4, 8.64×10^4 and 3.03×10^5 sec, respectively. In the early stage, isolated clouds are formed in ascent regions near 6 km height(Fig.3a, 4a). Thereafter, vertical velocity and cloud density increase, and the clouds grow up vertically(Fig.3b, 4b). Vertical velocity continues to increase until cloud distribution becomes horizontally uniform(Fig.3c, 4c), and thereafter becomes nearly constant temporally. After about 3.03×10^5 sec, the region above 7 km level is covered with clouds. One-cell circulation in which maximum vertical velocity is about 15 m/sec develops in the cloud layer. In the quasi-equilibrium state, around 7 km height, the cloud layer is sustained by the balance of negative contribution of evaporation and positive contribution of advection. At altitudes above 7 km, the cloud layer is sustained by the balance of negative contribution of advection and positive contribution of condensation.

Concluding Remarks

Our calculation shows that moist convection does develop in the case of $S_{cr} = 1.0$ (Fig.3b). This result is different from the discussion by Colaprete *et al*. (2003) that moist convection does not develop for $S_{cr} = 1.0$. In order to investigate the mechanism for development of the moist convection, detailed analysis will be required.

For further works, we are going to perform parameter sweep experiments for S_{cr}, and calculations with considering the falling of cloud particles. Since numerical experiments of cloud convection such as Nakajima *et al*.(1998) showed that the falling of cloud particles affects the convective structure, calculations with considering these effects are essential to investigate the structure of the convection which is established through a large number of life cycles of convective cloud elements.

Acknowledgement

Figures are plotted by using the softwares developed by Dennou Ruby Project (http://ruby.gfd-dennou.org/). Numerical calculations are performed by the SX8-R of the NIES supercomputer system.

References

Asselin, R., 1972: Frequency filter for time integrations, *Mon. Wea. Rev.*, **100**, 487–490.

Colaprete, A., Toon, O. B., 2002: Carbon dioxide snow storms during the polar night on Mars, *J. Geophys. Res.*, **107**, 5051, doi:10.1029/2001JE001758.

Colaprete, A., Haberle, R. M., Toon, O. B., 2003: Formation of convective carbon dioxide clouds near the south pole of Mars, *J. Geophys. Res.*, **108**(***E7***), 5081, doi:10.1029/2003JE002053

Forget, F., Pierrehumbert, R. T., 1997: Warming early Mars with carbon dioxide clouds that scatter infrared radiation, *Science*, **278**, 1273–1276.

Glandorf, D. L., Colaprete, A., Tolbert, M. A., Toon, O. B., 2002: CO_2 snow on Mars and early Earth: experimental constraints, *Icarus*, **160**, 66–72.

Kasting, J. F., 1991: CO_2 condensation and the climate of early Mars, *Icarus*, **94**, 1–13.

Klemp, J. B., Wilhelmson, R. B., 1978: The simulation of three-dimensional convective storm dynamics, *J. Atmos. Sci.*, **35**, 1070–1096.

Mitsuda, C., 2007: The greenhouse effect of radiatively adjusted CO_2 ice cloud in a Martian paleoatmosphere (in Japanese), Doctoral thesis, Hokkaido Univ.,115pp.

Nakajima, K., Takehiro, S., Ishiwatari, M., Hayashi,Y.-Y., 1998: Cloud convections in geophysical and planetary fluids(in Japanese), *Nagare Multi.*, http://www2.nagare.or.jp/mm/98/nakajima/index.htm

Nakajima, K., Takehiro, S., Ishiwatari, M., Hayashi,Y.-Y., 2000: Numerical modeling of Jupiter's moist convection layer, *Geophys. Res. Lett.*, **27**, 3129–3132.

National Astronomical Observatory of Japan, 2004: Chronological scientific tables (in Japanese), *Maruzen*, 1015pp.

Odaka, M., Kitamori, T., Sugiyama, K., Nakajima, K., Takahashi, Y. O., Ishiwatari, M., Hayashi, Y.-Y., 2005: A formulation of non-hydrostatic model for moist convection in the Martian atmosphere, Proc. of the 38 th ISAS Lunar and Planetary Symposium, 173–175.

Odaka, M., Kitamori, T., Sugiyama, K., Nakajima, K., Hayashi, Y.-Y., 2006: A numerical simulation of Martian atmospheric moist convection (in Japanese), Proc. of the 20 th ISAS Atmospheric Science Symposium, 103–106.

Pollack, J. B, Kasting, J. F., Richardson, S. M. and Poliakoff. K., 1987: The case for a wet, warm climate on early Mars, *Icarus*, **71**, 203–224.

Sugiyama, K., Odaka, M., Nakajima, K., Hayashi, Y.-Y., 2009: Development of a cloud convection model to investigate the Jupiter's atmosphere, *Nagare Multi.*, http://www2.nagare.or.jp/mm/2009/sugiyama/index.htm

The society of chemical engineers of Japan, 1999: The handbook of chemistry and engineering (in Japanese), *Maruzen*, 1339 pp.

Tobie, G., Forget, F., Lott, F., 2003: Numerical simulation of winter polar wave clouds observed by Mars Global Surveyor Mars Orbiter Laser Altimeter, *Icarus*, **35**, 33–49.

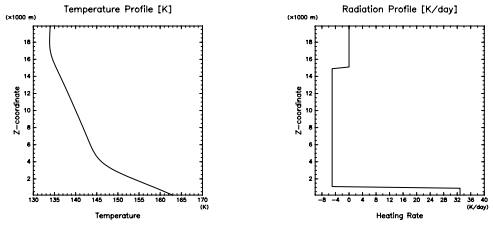

Figure 1: Initial temperature profile (left panel) and initial profile of heating rate(right panel).

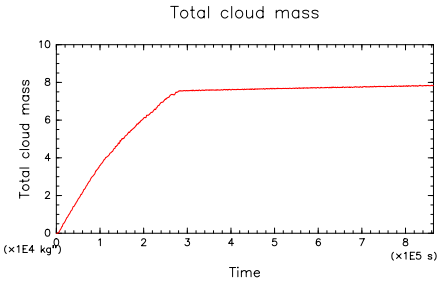

Figure 2: Time evolution of total cloud mass from 0 sec to 8.64×10^5 sec.

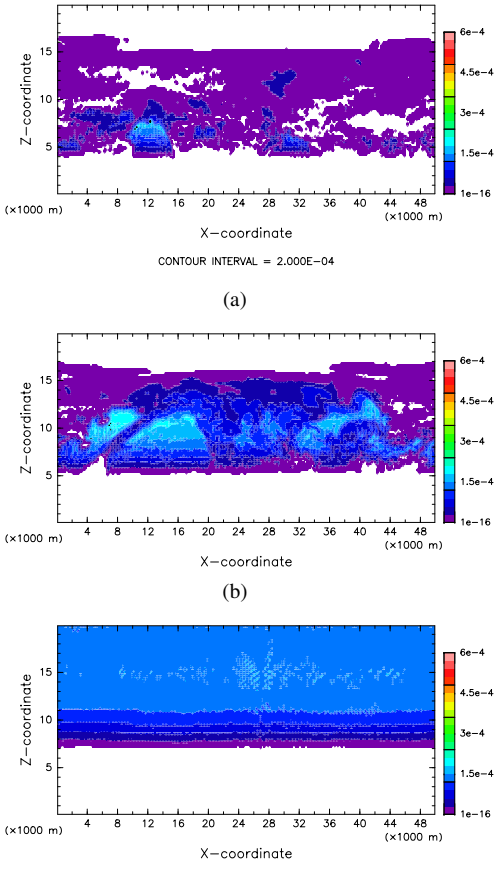

Figure 3: Snapshots for distribution of density of cloud [kg/m^3] at : (a) 2.16×10^4 sec, (b) 8.64×10^4 sec, (c) 3.03×10^5 sec.

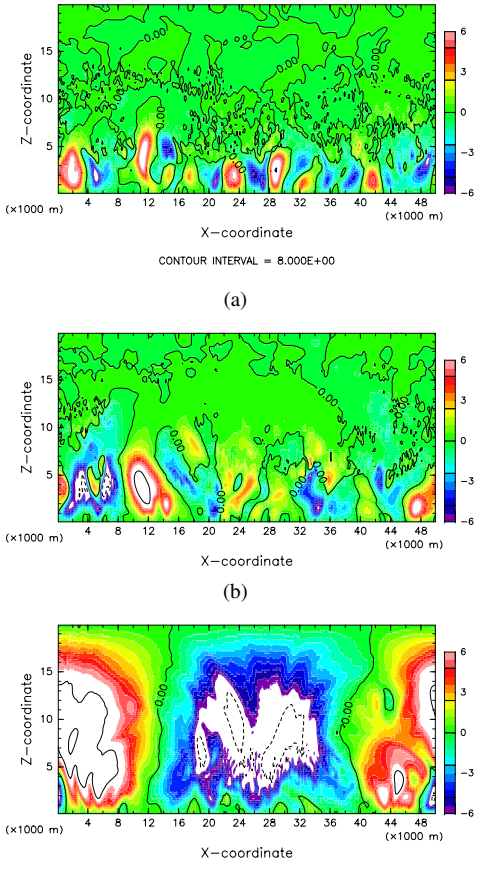

Figure 4: Snapshots for distribution of vertical velocity [m/sec] at : (a) 2.16×10^4 sec, (b) 8.64×10^4 sec, (c) 3.03×10^5 sec.